

## Deterministic photonic quantum computation in a synthetic time dimension: supplement

**BEN BARTLETT,<sup>1,2,3</sup>  AVIK DUTT,<sup>2</sup>  AND SHANHUI FAN<sup>2,\*</sup> **

<sup>1</sup>*Department of Applied Physics, Stanford University, Stanford, California 94305, USA*

<sup>2</sup>*Department of Electrical Engineering, Stanford University, Stanford, California 94305, USA*

<sup>3</sup>*e-mail: [benbartlett@stanford.edu](mailto:benbartlett@stanford.edu)*

*\*Corresponding author: [shanhui@stanford.edu](mailto:shanhui@stanford.edu)*

---

This supplement published with Optica Publishing Group on 29 November 2021 by The Authors under the terms of the [Creative Commons Attribution 4.0 License](https://creativecommons.org/licenses/by/4.0/) in the format provided by the authors and unedited. Further distribution of this work must maintain attribution to the author(s) and the published article's title, journal citation, and DOI.

Supplement DOI: <https://doi.org/10.6084/m9.figshare.16862155>

Parent Article DOI: <https://doi.org/10.1364/OPTICA.424258>

# Deterministic photonic quantum computation in a synthetic time dimension: supplementary information

In this Supplementary Information document, we give more detailed presentations of the results described in the main paper. In Section 1 we present a derivation of the gate teleportation mechanism; in Section 2 we derive a method to construct arbitrary single-qubit operations from the teleported gates; in Section 3 we construct a photon-atom SWAP operation from scattering sequences and measurement; in Section 4 we describe constructions for a two-photon  $c\sigma_z$  gate; in Section 5 we give more detail of the circuit compilation process and provide an example of a compiled instruction sequence to implement a quantum Fourier transform on our proposed device; and in Section 6 we discuss in greater detail the imperfection analysis described in the main text.

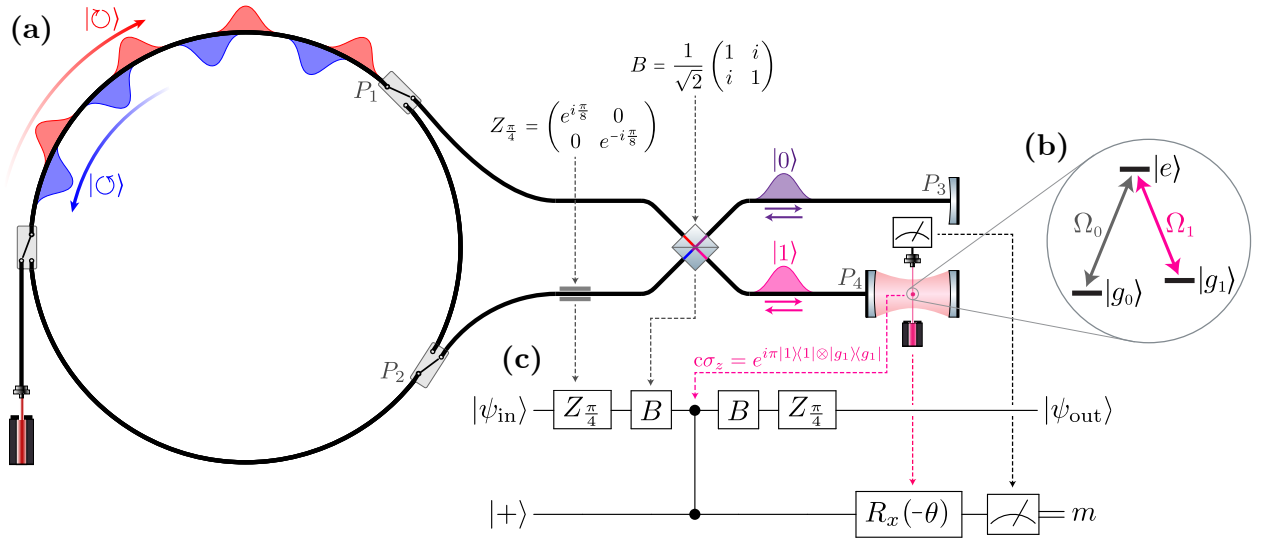


**Fig. S1.** An annotated figure depicting the architecture described in the main text and the correspondence of physical and logical circuit elements. (a) The physical design of the device, with annotations indicating quantum operations implemented by physical circuit elements. (b) The energy structure of the atom:  $\Omega_1$  is resonant with the cavity mode and photon carrier frequency, while  $\Omega_0$  is far-detuned. (c) Gate diagram of the quantum circuit applied in a single pass of a photonic qubit through the scattering unit. The top rail denotes the state of the photonic qubit and the bottom rail denotes the atomic qubit. After the photon returns to the storage ring,  $R_x(-\theta)$  is applied to the atomic qubit and a projective measurement of the atomic state is performed. The final output state  $|\psi_{out}\rangle$  is  $Z_{\pi/4}\sigma_z(-\sigma_y)^{m\oplus 1}R_y(\theta)Z_{\pi/4}|\psi_{in}\rangle$ , as described in Eq. 2 of the main text.

## 1. DERIVATION OF GATE TELEPORTATION MECHANISM

Consider a photon which is circulating in the storage ring in a state  $|\psi_{in}\rangle = \alpha|0\rangle + \beta|1\rangle$ , where  $|0\rangle$  and  $|1\rangle$  denote the two counter-propagating states. Referring to Figure S1, define bosonic operators  $\hat{a}_{\circ}^{\dagger}(t)$ ,  $\hat{a}_{\ominus}^{\dagger}(t)$  which create at time  $t$  a clockwise- or counterclockwise-propagating photon in the ring at the points  $P_1$ ,  $P_2$ , respectively, just before the switches. The physical state of the photon in the ring can be written as

$$|\psi_{in}\rangle = \int dt \phi(t) \left[ \alpha \hat{a}_{\circ}^{\dagger}(t) + \beta \hat{a}_{\ominus}^{\dagger}(t) \right] |\emptyset\rangle, \quad (\text{S1})$$

where  $|\emptyset\rangle$  denotes the vacuum state and  $\phi(t)$  describes the pulse envelope. Here we assume that the photon was originally injected in the  $|0\rangle$  state as shown in Figure S1 and has undergone at most a small number of scattering interactions with the atom-cavity system, such that the clockwise and counterclockwise pulses have not independently deformed significantly and can be described by a single envelope.

We also define bosonic operators  $\hat{b}_{0,d}^{\dagger}(t)$ ,  $\hat{b}_{1,d}^{\dagger}(t)$  which respectively create a photon in the top or bottom waveguides at points  $P_1$ ,  $P_2$  at time  $t$  propagating with direction  $d \in \{L, R\}$ . As the photon is injected by the switches from the ring into the waveguides, the fixed  $\pi/4$  phase shifter applies (up to a global phase) a rotation  $Z_{\pi/4} \equiv R_z(\pi/4) = \begin{pmatrix} e^{-i\pi/8} & 0 \\ 0 & e^{i\pi/8} \end{pmatrix}$  to

the photon state, and the beamsplitter applies the operation  $B = \frac{1}{\sqrt{2}} \begin{pmatrix} 1 & i \\ i & 1 \end{pmatrix}$ . Finally, let operators  $\hat{c}_{0,d}^\dagger(t), \hat{c}_{1,d}^\dagger(t)$  with  $d \in \{L, R\}$  create a photon at time  $t$  in the top or bottom waveguides just before the mirror or cavity at points  $P_3$  and  $P_4$ .

The round trip distance from points  $P_1, P_2$  to  $P_3, P_4$  and back is equal to the ring circumference  $L = n\Delta t$ , where the speed of light in the waveguides is set to unity and where  $n$  is the number of time bins. This matching path length ensures that a photon which leaves the ring to scatter against the atom will return to its original time bin. Let time  $t_0$  denote the point at which the clockwise and counterclockwise components of the photon in the ring pass their respective switches and may be injected into the scattering unit. When the switches are set to the open state, we can relate the  $\hat{a}^\dagger, \hat{b}^\dagger, \hat{c}^\dagger$  operators on the outgoing pass of the photon with:

$$\begin{bmatrix} \hat{b}_{0,R}^\dagger(t_0) \\ \hat{b}_{1,R}^\dagger(t_0) \end{bmatrix} = \begin{bmatrix} \hat{a}_\odot^\dagger(t) \\ \hat{a}_\ominus^\dagger(t) \end{bmatrix}, \quad \begin{bmatrix} \hat{c}_{0,R}^\dagger(t_0 + \frac{n\Delta t}{2}) \\ \hat{c}_{1,R}^\dagger(t_0 + \frac{n\Delta t}{2}) \end{bmatrix} = BZ_{\frac{\pi}{4}} \begin{bmatrix} \hat{b}_{0,R}^\dagger(t) \\ \hat{b}_{1,R}^\dagger(t) \end{bmatrix}. \quad (\text{S2})$$

The  $\hat{c}_{1,R}^\dagger$  component of the photon interacts at time  $t_1 = t_0 + \frac{n\Delta t}{2}$  with the  $|g_1\rangle$  component of the atomic state that is resonant with the photon frequency, applying the unitary transformation onto the joint photon-atom state  $c\sigma_z = e^{i\pi|1\rangle\langle 1| \otimes |g_1\rangle\langle g_1|} = \exp(i\pi \hat{c}_{1,R}^\dagger |\emptyset\rangle\langle \emptyset| \hat{c}_{1,R} \otimes |g_1\rangle\langle g_1|)$ . Thus, we can relate the operators before and after reflection/scattering as:

$$\left( \begin{bmatrix} \hat{c}_{0,L}^\dagger(t_1) \\ \hat{c}_{1,L}^\dagger(t_1) \end{bmatrix} \otimes \begin{bmatrix} |g_0\rangle\langle g_0| \\ |g_1\rangle\langle g_1| \end{bmatrix} \right) = \exp(i\pi \hat{c}_{1,R}^\dagger(t_1) \hat{c}_{1,R}(t_1) \otimes |g_1\rangle\langle g_1|) \left( \begin{bmatrix} \hat{c}_{0,R}^\dagger(t_1) \\ \hat{c}_{1,R}^\dagger(t_1) \end{bmatrix} \otimes \begin{bmatrix} |g_0\rangle\langle g_0| \\ |g_1\rangle\langle g_1| \end{bmatrix} \right), \quad (\text{S3})$$

where we assume that the interaction timescale (usually set by the cavity lifetime) is negligible compared to the time bin size  $\Delta t$  (the long pulse limit). Eq. S3 is derived for scattering in the single-photon subspace, but is applicable to multi-photon states as long as the photon wavefunctions do not overlap in the scattering unit.

On the return trip, after scattering against the atom, the photon passes through the beamsplitter and phase shifter in reverse order before being re-injected at time  $t_2 = t_1 + \frac{n\Delta t}{2}$  into the ring at points  $P_1, P_2$ , allowing us to relate the final set of operators:

$$\begin{bmatrix} \hat{b}_{0,L}^\dagger(t_2) \\ \hat{b}_{1,L}^\dagger(t_2) \end{bmatrix} = Z_{\frac{\pi}{4}}^\dagger B^\dagger \begin{bmatrix} \hat{c}_{0,L}^\dagger(t_1) \\ \hat{c}_{1,L}^\dagger(t_1) \end{bmatrix}, \quad \begin{bmatrix} \hat{a}_\odot^\dagger(t_2) \\ \hat{a}_\ominus^\dagger(t_2) \end{bmatrix} = \begin{bmatrix} \hat{b}_{0,L}^\dagger(t_2) \\ \hat{b}_{1,L}^\dagger(t_2) \end{bmatrix}. \quad (\text{S4})$$

Note that the  $\hat{a}^\dagger$  and  $\hat{b}^\dagger$  operators have opposite couplings on the photon's return trip; e.g. the clockwise  $\hat{a}_\odot^\dagger$  operator couples to the top waveguide  $\hat{b}_{0,R}^\dagger$  on the outgoing direction, while on the return trip, the top waveguide  $\hat{b}_{0,L}^\dagger$  couples to the counterclockwise mode  $\hat{a}_\ominus^\dagger$ . One can combine the equations above to obtain that, if the atom is in the non-interacting state  $|g_0\rangle$ , the total transformation performed on the photon by a round trip through the scattering unit is  $Z_{\frac{\pi}{4}} B B Z_{\frac{\pi}{4}}$ , and the photon state in the ring is unchanged up to a factor of  $i$ :  $\hat{a}_\odot^\dagger(t + n\Delta t) = i\hat{a}_\odot^\dagger(t)$  and  $\hat{a}_\ominus^\dagger(t + n\Delta t) = i\hat{a}_\ominus^\dagger(t)$ .

For the purpose of the gate teleportation, we initialize the atom in the  $|g_0\rangle$  state and use a  $R_y(\pi/2)$  rotation to change the state to  $|+\rangle \equiv \frac{1}{\sqrt{2}}(|g_0\rangle + |g_1\rangle)$ . The scattering interaction applies a  $\pi$  phase shift to the  $|1\rangle \otimes |g_1\rangle$  component of the joint quantum state, implementing a  $c\sigma_z$  gate. After the photon has interacted with the atom, an  $R_x(-\theta)$  rotation is applied to the atom as the photon passes back through the beamsplitter and phase shifter and is injected back into the ring. Thus, the joint photon-atom state after scattering is:

$$|\Phi\rangle = \left( (Z_{\frac{\pi}{4}} B) \otimes R_x(-\theta) \right) c\sigma_z \left( (B Z_{\frac{\pi}{4}}) \otimes R_y(\pi/2) \right) (|\psi_{\text{in}}\rangle \otimes |g_0\rangle). \quad (\text{S5})$$

Finally, a projective measurement of the atom's state in the  $\{|g_0\rangle, |g_1\rangle\}$  basis is performed, obtaining a bit  $m \in \{0, 1\}$ . If the atomic state collapses to state  $|g_m\rangle$ , then we obtain a disentangled output photon-atom state:

$$|\psi_{\text{out}}\rangle \otimes |g_m\rangle = \frac{1}{\sqrt{P_m}} [\mathbb{1} \otimes |g_m\rangle\langle g_m|] |\Phi\rangle, \quad (\text{S6})$$

where  $P_m = \text{tr}[(\mathbb{1} \otimes |g_m\rangle\langle g_m|)|\Phi\rangle\langle\Phi|]$ . Working in the long pulse, high cooperativity limit where pulse shape deformation from the scattering interaction is negligible<sup>1</sup>, we obtain respective output states for  $m = 0, 1$  of:

$$|\psi_{\text{out}}\rangle \otimes |g_0\rangle = \int dt \phi(t) \left[ \left( i\beta \cos \frac{\theta}{2} + e^{-\frac{i\pi}{4}} \alpha \sin \frac{\theta}{2} \right) \hat{a}_\odot^\dagger(t) + \left( i\alpha \cos \frac{\theta}{2} + e^{-\frac{i\pi}{4}} \beta \sin \frac{\theta}{2} \right) \hat{a}_\ominus^\dagger(t) \right] |\emptyset\rangle \otimes |g_0\rangle \quad (\text{S7})$$

$$|\psi_{\text{out}}\rangle \otimes |g_1\rangle = \int dt \phi(t) \left[ \left( e^{-\frac{i\pi}{4}} \alpha \cos \frac{\theta}{2} - \beta \sin \frac{\theta}{2} \right) \hat{a}_\odot^\dagger(t) - \left( e^{-\frac{i\pi}{4}} \beta \cos \frac{\theta}{2} + \alpha \sin \frac{\theta}{2} \right) \hat{a}_\ominus^\dagger(t) \right] |\emptyset\rangle \otimes |g_1\rangle, \quad (\text{S8})$$

<sup>1</sup>Here we assume that the temporal pulse length  $\tau$  is much less than the time bin spacing  $\Delta t$  but significantly larger than the cavity decay rate, such that the pulse shape changes slowly compared to the cavity decay rate. This means that the pulse shapes for the clockwise and counterclockwise components of the photon state do not change independently. A more realistic treatment of the pulse deformation is given in the imperfection analysis presented here and in the main text.

with  $\alpha, \beta$  the coefficients from the input state of Eq. S1. Thus, the output photon state  $|\psi_{\text{out}}\rangle$ , depending on the outcome of the atomic measurement  $m$ , is:

$$|\psi_{\text{out}}\rangle = \begin{cases} -iZ_{\frac{\pi}{4}}\sigma_z R_y(\theta + \pi)Z_{\frac{\pi}{4}}|\psi_{\text{in}}\rangle & \text{if } m = 0 \\ Z_{\frac{\pi}{4}}\sigma_z R_y(\theta)Z_{\frac{\pi}{4}}|\psi_{\text{in}}\rangle & \text{if } m = 1 \end{cases} \quad (\text{S9})$$

$$= Z_{\frac{\pi}{4}}\sigma_z (-\sigma_y)^{m\oplus 1} R_y(\theta) Z_{\frac{\pi}{4}}|\psi_{\text{in}}\rangle,$$

where  $m \oplus 1$  denotes addition modulo 2.

## 2. CONSTRUCTING ARBITRARY SINGLE-QUBIT ROTATIONS

To construct arbitrary single-qubit gates, we compose a sequence of teleported gates of the form in Eq. S9 with a sequence of “non-entangling” scattering process which correct for local Pauli errors introduced depending on the atomic measurement outcomes. If the atom is initialized to the off-resonant  $|g_0\rangle$  state, then the atom-cavity system is on resonance with the incident photon and behaves as a mirror. In this case, the  $\pi$  phase shifts imparted by the cavity and by the mirror in the top waveguide cancel, and the photon state is transformed as  $|\psi_{\text{out}}\rangle = Z_{\frac{\pi}{4}}BBZ_{\frac{\pi}{4}}|\psi_{\text{in}}\rangle = i\sigma_x|\psi_{\text{in}}\rangle$ . If the atom is initialized to  $|g_1\rangle$ , then the atom-cavity system is off resonance with the incident photon. In this case, the phase shift from the mirror in the top waveguide is not matched and a relative  $\pi$  phase shift is imparted between the top and bottom modes, transforming the photon state as  $|\psi_{\text{out}}\rangle = Z_{\frac{\pi}{4}}B\sigma_zBZ_{\frac{\pi}{4}}|\psi_{\text{in}}\rangle = -i\sigma_zZ_{\pi/2}|\psi_{\text{in}}\rangle$ .

Now consider a sequence of three successive teleported rotation gates  $R_y(\theta_1), R_y(\theta_2), R_y(\theta_3)$ , with atomic measurement results  $m_1, m_2, m_3$ . The goal here is to create a sequence of scattering operations which result in a gate of the form  $U = R_y(\theta_3)R_x(\theta_2)R_y(\theta_1)$ , which is sufficient to implement any single-qubit gate up to an overall phase decomposed as Euler angles. [1] The total operation  $U$  applied to the initial input state  $|\psi_{\text{in}}\rangle$  from the three scattering operations is:

$$U = (-1)^{m_1\oplus m_2\oplus m_3\oplus 1} Z_{\frac{\pi}{4}}\sigma_z(\sigma_y)^{m_3\oplus 1} R_y(\theta_3)Z_{\frac{\pi}{4}}Z_{\frac{\pi}{4}}\sigma_z(\sigma_y)^{m_2\oplus 1} R_y(\theta_2)Z_{\frac{\pi}{4}}Z_{\frac{\pi}{4}}\sigma_z(\sigma_y)^{m_1\oplus 1} R_y(\theta_1)Z_{\frac{\pi}{4}}. \quad (\text{S10})$$

We can simplify this expression by noting that  $Z_{\frac{\pi}{4}}Z_{\frac{\pi}{4}}\sigma_z(\sigma_y)^{m\oplus 1} = -i(-i\sigma_y\sigma_z)^{m\oplus 1}Z_{-\frac{\pi}{2}} = -i(\sigma_x)^{m\oplus 1}Z_{-\frac{\pi}{2}}$ , which reduces Eq. S10 to:

$$U = (-1)^{m_3\oplus m_2\oplus m_1} (-i)^{m_2\oplus m_1} Z_{\frac{\pi}{4}}\sigma_z(\sigma_y)^{m_3\oplus 1} R_y(\theta_3)(\sigma_y\sigma_z)^{m_2\oplus 1} Z_{-\frac{\pi}{2}} R_y(\theta_2)(\sigma_y\sigma_z)^{m_1\oplus 1} Z_{-\frac{\pi}{2}} R_y(\theta_1)Z_{\frac{\pi}{4}}. \quad (\text{S11})$$

Since the results of previous measurements can add extraneous Pauli gates which affect future rotations, we wish to perform adaptive operations based on the measured outcomes. After the first measurement  $m_1$  is performed, the gate operation is:

$$U = \begin{cases} (-1)^{m_3\oplus m_2} (-i)^{m_2} Z_{\frac{\pi}{4}}\sigma_z(\sigma_y)^{m_3\oplus 1} R_y(\theta_3)(\sigma_y\sigma_z)^{m_2\oplus 1} Z_{-\frac{\pi}{2}} R_y(\theta_2)\sigma_y\sigma_z Z_{-\frac{\pi}{2}} R_y(\theta_1)Z_{\frac{\pi}{4}} & \text{if } m_1 = 0 \\ (-1)^{m_3\oplus m_2\oplus 1} (-i)^{m_2\oplus 1} Z_{\frac{\pi}{4}}\sigma_z(\sigma_y)^{m_3\oplus 1} R_y(\theta_3)(\sigma_y\sigma_z)^{m_2\oplus 1} Z_{-\frac{\pi}{2}} R_y(\theta_2)Z_{-\frac{\pi}{2}} R_y(\theta_1)Z_{\frac{\pi}{4}} & \text{if } m_1 = 1. \end{cases} \quad (\text{S12})$$

Using the identities that  $\sigma_z Z_{-\frac{\pi}{2}} = iZ_{+\frac{\pi}{2}}$  and that  $R_i(\theta)\sigma_i = -iR_i(\theta + \pi)$  for  $i = x, y, z$ , we can rewrite this as:

$$U = \begin{cases} (-1)^{m_3\oplus m_2} (-i)^{m_2} Z_{\frac{\pi}{4}}\sigma_z(\sigma_y)^{m_3\oplus 1} R_y(\theta_3)(\sigma_y\sigma_z)^{m_2\oplus 1} Z_{-\frac{\pi}{2}} R_y(\theta_2 + \pi)Z_{+\frac{\pi}{2}} R_y(\theta_1)Z_{\frac{\pi}{4}} & \text{if } m_1 = 0 \\ (-1)^{m_3\oplus m_2\oplus 1} (-i)^{m_2\oplus 1} Z_{\frac{\pi}{4}}\sigma_z(\sigma_y)^{m_3\oplus 1} R_y(\theta_3)(\sigma_y\sigma_z)^{m_2\oplus 1} Z_{-\frac{\pi}{2}} R_y(\theta_2)Z_{-\frac{\pi}{2}} R_y(\theta_1)Z_{\frac{\pi}{4}} & \text{if } m_1 = 1. \end{cases} \quad (\text{S13})$$

Substituting  $Z_{-\frac{\pi}{2}}R_y(\theta)Z_{+\frac{\pi}{2}} = R_x(\theta)$  and  $Z_{-\frac{\pi}{2}}R_y(\theta)Z_{-\frac{\pi}{2}} = i\sigma_zR_x(-\theta)$ , we rearrange the equation to turn the second rotation gate into a  $R_x(\pm\theta)$  gate, where the sign depends on the outcome of  $m_1$ , which is already known:

$$U = \begin{cases} (-1)^{m_3\oplus m_2} (-i)^{m_2} Z_{\frac{\pi}{4}}\sigma_z(\sigma_y)^{m_3\oplus 1} R_y(\theta_3)(\sigma_y\sigma_z)^{m_2\oplus 1} R_x(\theta_2 + \pi)R_y(\theta_1)Z_{\frac{\pi}{4}} & \text{if } m_1 = 0 \\ i(-1)^{m_3\oplus m_2\oplus 1} (-i)^{m_2\oplus 1} Z_{\frac{\pi}{4}}\sigma_z(\sigma_y)^{m_3\oplus 1} R_y(\theta_3)(\sigma_y\sigma_z)^{m_2\oplus 1} \sigma_z R_x(-\theta_2)R_y(\theta_1)Z_{\frac{\pi}{4}} & \text{if } m_1 = 1 \end{cases} \quad (\text{S14})$$

$$= (-1)^{m_3} Z_{\frac{\pi}{4}}\sigma_z(\sigma_y)^{m_3\oplus 1} R_y(\theta_3)(i\sigma_y\sigma_z)^{m_2\oplus 1} \times \begin{cases} R_x(\theta_2 + \pi)R_y(\theta_1)Z_{\frac{\pi}{4}} & \text{if } m_1 = 0 \\ \sigma_z R_x(-\theta_2)R_y(\theta_1)Z_{\frac{\pi}{4}} & \text{if } m_1 = 1. \end{cases}$$

Importantly, the decision for which adaptive changes to apply to the  $\theta_2$  operation (adding  $\pi$  or inverting the angle) can be made knowing only the outcome of the previous measurement  $m_1$ . Let  $\theta_2(m_1) = \theta_2 + \pi$  if  $m_1 = 0$  and  $-\theta_2$  if  $m_1 = 1$  denote the adaptive angle to implement the desired rotation  $R_x(\theta_2)$ . Then we can rewrite Eq. S14 as:

$$U = (-1)^{m_3} Z_{\frac{\pi}{4}}\sigma_z(\sigma_y)^{m_3\oplus 1} R_y(\theta_3)(i\sigma_y\sigma_z)^{m_2\oplus 1} \sigma_z^{m_1} R_x(\theta_2(m_1)) R_y(\theta_1)Z_{\frac{\pi}{4}}. \quad (\text{S15})$$

We repeat this process of performing a measurement and commuting the error terms to the front of the equation for measurement  $m_2$ . After performing the second measurement, we use  $R_y(\theta)\sigma_z = \sigma_z R_y(-\theta)$  and the above identities to obtain:

$$\begin{aligned}
U &= (-1)^{m_3} Z_{\frac{\pi}{4}} \sigma_z (\sigma_y)^{m_3 \oplus 1} R_y(\theta_3) \times \begin{cases} i\sigma_y \sigma_z R_x(\theta_2(m_1)) R_y(\theta_1) Z_{\frac{\pi}{4}} & \text{if } m_1 = 0, m_2 = 0 \\ R_x(\theta_2(m_1)) R_y(\theta_1) Z_{\frac{\pi}{4}} & \text{if } m_1 = 0, m_2 = 1 \\ i\sigma_y \sigma_z \sigma_z R_x(\theta_2(m_1)) R_y(\theta_1) Z_{\frac{\pi}{4}} & \text{if } m_1 = 1, m_2 = 0 \\ \sigma_z R_x(\theta_2(m_1)) R_y(\theta_1) Z_{\frac{\pi}{4}} & \text{if } m_1 = 1, m_2 = 1 \end{cases} \\
&= (-1)^{m_3} Z_{\frac{\pi}{4}} \sigma_z (\sigma_y)^{m_3 \oplus 1} \times \begin{cases} -R_y(\theta_3 + \pi) \sigma_z R_x(\theta_2(m_1)) R_y(\theta_1) Z_{\frac{\pi}{4}} & \text{if } m_1 = 0, m_2 = 0 \\ R_y(\theta_3) R_x(\theta_2(m_1)) R_y(\theta_1) Z_{\frac{\pi}{4}} & \text{if } m_1 = 0, m_2 = 1 \\ -R_y(\theta_3 + \pi) R_x(\theta_2(m_1)) R_y(\theta_1) Z_{\frac{\pi}{4}} & \text{if } m_1 = 1, m_2 = 0 \\ R_y(\theta_3) \sigma_z R_x(\theta_2(m_1)) R_y(\theta_1) Z_{\frac{\pi}{4}} & \text{if } m_1 = 1, m_2 = 1 \end{cases} \quad (S16) \\
&= (-1)^{m_3} Z_{\frac{\pi}{4}} \sigma_z (\sigma_y)^{m_3 \oplus 1} \times \begin{cases} -\sigma_z R_y(-\theta_3 - \pi) R_x(\theta_2(m_1)) R_y(\theta_1) Z_{\frac{\pi}{4}} & \text{if } m_1 = 0, m_2 = 0 \\ R_y(\theta_3) R_x(\theta_2(m_1)) R_y(\theta_1) Z_{\frac{\pi}{4}} & \text{if } m_1 = 0, m_2 = 1 \\ -R_y(\theta_3 + \pi) R_x(\theta_2(m_1)) R_y(\theta_1) Z_{\frac{\pi}{4}} & \text{if } m_1 = 1, m_2 = 0 \\ \sigma_z R_y(-\theta_3) R_x(\theta_2(m_1)) R_y(\theta_1) Z_{\frac{\pi}{4}} & \text{if } m_1 = 1, m_2 = 1. \end{cases}
\end{aligned}$$

As before, the modifications to  $\theta_3$  can be performed with only knowledge of  $m_1$  and  $m_2$ . Let  $\theta_3(m_2, m_1)$  be defined as in the four cases of Eq. S16, such that  $\theta_3(m_2, m_1) = (-1)^{m_2 \oplus m_2 \oplus 1} (\theta_3 + \pi(1 - m_2))$ . We perform the final measurement  $m_3$  using this adaptive  $\theta_3$ . We obtain an equation of the desired form with a possible Pauli error term  $\epsilon(m_1, m_2, m_3)$  at the front:

$$\begin{aligned}
U &= (-1)^{m_3} Z_{\frac{\pi}{4}} \sigma_z (\sigma_y)^{m_3 \oplus 1} (-1)^{m_2} \sigma_z^{m_2 \oplus m_1 \oplus 1} R_y(\theta_3(m_2, m_1)) R_x(\theta_2(m_1)) R_y(\theta_1) Z_{\frac{\pi}{4}} \\
&= (-1)^{m_3 \oplus m_2 \oplus 1} Z_{\frac{\pi}{4}} \sigma_z^{m_2 \oplus m_1} (\sigma_y)^{m_3 \oplus 1} R_y(\theta_3(m_2, m_1)) R_x(\theta_2(m_1)) R_y(\theta_1) Z_{\frac{\pi}{4}} \\
&= (-1)^{m_3 \oplus m_2 \oplus 1} \sigma_z^{m_2 \oplus m_1} (-\sigma_y)^{m_3 \oplus 1} Z_{\frac{\pi}{4}} R_y(\theta_3(m_2, m_1)) R_x(\theta_2(m_1)) R_y(\theta_1) Z_{\frac{\pi}{4}} \\
&\equiv \epsilon(m_1, m_2, m_3) Z_{\frac{\pi}{4}} R_y(\theta_3(m_2, m_1)) R_x(\theta_2(m_1)) R_y(\theta_1) Z_{\frac{\pi}{4}},
\end{aligned} \quad (S17)$$

where the error term  $\epsilon(m_1, m_2, m_3)$  is:

$$\begin{aligned}
\epsilon(0, 0, 0) &= -\sigma_y \\
\epsilon(0, 0, 1) &= -\mathbb{1} \\
\epsilon(0, 1, 0) &= -i\sigma_x \\
\epsilon(0, 1, 1) &= \sigma_z \\
\epsilon(1, 0, 0) &= -i\sigma_x \\
\epsilon(1, 0, 1) &= \sigma_z \\
\epsilon(1, 1, 0) &= -\sigma_y \\
\epsilon(1, 1, 1) &= -\mathbb{1}.
\end{aligned} \quad (S18)$$

We can remove any of these errors up to a global phase by using a sequence of non-interacting passes, where the atom is initialized to  $|g_0\rangle$  or  $|g_1\rangle$  rather than  $|+\rangle$ . To remove  $-i\sigma_x$ , we use a  $|g_0\rangle$  initialization to apply  $Z_{\frac{\pi}{4}} B B Z_{\frac{\pi}{4}} = i\sigma_x$ . To remove  $\sigma_z$ , we use two  $|g_1\rangle$ -initialized scatterings to apply  $Z_{\frac{\pi}{4}} B \sigma_z B Z_{\frac{\pi}{4}} Z_{\frac{\pi}{4}} B \sigma_z B Z_{\frac{\pi}{4}} = -i\sigma_z$ . To remove  $\sigma_y$ , we apply two  $|g_1\rangle$ -initialized scatterings and one  $|g_0\rangle$ -initialized scatterings to apply  $Z_{\frac{\pi}{4}} B \sigma_z B Z_{\frac{\pi}{4}} Z_{\frac{\pi}{4}} B \sigma_z B Z_{\frac{\pi}{4}} B B Z_{\frac{\pi}{4}} = -i\sigma_y$ . Thus, one can apply arbitrary single-qubit operations parameterized via YXY Euler angles using this gate construction method.

### 3. PHOTONIC QUBIT READOUT

To measure the state of a photonic qubit, we construct a SWAP gate from a sequence of three scattering operations. We may initialize the atom to any state, and we then perform the sequence of scattering interactions shown in Figure S2.

Let  $|\psi\rangle = (\alpha \hat{b}_{0L}^\dagger + \beta \hat{b}_{1L}^\dagger) |\varnothing\rangle$  be the state of the photon at points  $P_3, P_4$  in the device. By scattering the photon against the atom three times and applying the rotation  $R_y(\pi/2)R_x(\pi)$  to the atomic states in between scattering, one can swap

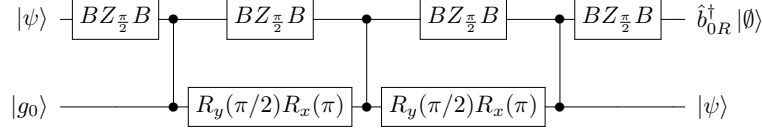


**Fig. S2.** Construction of a SWAP gate from three scattering interactions. The top rail denotes the photonic qubit and the bottom rail denotes the atom. The  $BZ_{\frac{\pi}{2}}B$  operations correspond to a return trip of the photon from the scattering site to the ring and back, passing through the beamsplitter and phase shifter twice.

the states of the photon and atom, such that the final atomic state is  $\alpha |g_0\rangle + \beta |g_1\rangle$ . It is straightforward to verify that this sequence of operations implements the SWAP gate up to a phase of -1:

$$\left(BZ_{\frac{\pi}{2}}B \otimes \mathbb{1}\right) c\sigma_z \left(BZ_{\frac{\pi}{2}}B \otimes Y_{\frac{\pi}{2}} X_{\pi}\right) c\sigma_z \left(BZ_{\frac{\pi}{2}}B \otimes Y_{\frac{\pi}{2}} X_{\pi}\right) c\sigma_z \left(BZ_{\frac{\pi}{2}}B \otimes \mathbb{1}\right) = -1 \begin{pmatrix} 1 & 0 & 0 & 0 \\ 0 & 0 & 1 & 0 \\ 0 & 1 & 0 & 0 \\ 0 & 0 & 0 & 1 \end{pmatrix}. \quad (\text{S19})$$

Once the states of the photonic and atomic qubits are swapped, the atomic state can be measured with near 100% efficiency using the quantum jump technique [2, 3] while the photonic qubit is discarded by allowing it to gradually dissipate through leakage to the environment. This SWAP-and-measure protocol can be repeated for the rest of the photonic qubits to read out the entire photonic quantum state.

#### 4. IMPLEMENTING A TWO-PHOTON $c\sigma_z$ GATE

In addition to implementing single-qubit gates, constructing a two-photon entangling gate is necessary for universal computation. A controlled phase-flip gate  $c\sigma_z$  between two photonic qubits can be constructed through a sequence of three scattering interactions in a somewhat similar manner as in Ref. [3]. However, the fixed beamsplitter and phase shifter, which are required for implementation of single-qubit gates in our scheme, only allow us to apply operations of the form  $\left(Z_{\frac{\pi}{4}}B \otimes \mathbb{1}\right) c\sigma_z \left(BZ_{\frac{\pi}{4}} \otimes \mathbb{1}\right)$  to the  $|\text{photon}\rangle \otimes |\text{atom}\rangle$  system with each scattering interaction. This prevents us from performing the exact protocol described in Ref. [3], which requires photons to undergo three successive  $c\sigma_z$  operations without any gates between them.

Here we describe two possible implementations of this  $c\sigma_z$  gate between two photons  $A$  and  $B$  in states  $|\psi_A\rangle$  and  $|\psi_B\rangle$  which work with the design of our proposed device. The first solution is to use a SWAP gate as described in Section 3 to swap the states of photon  $A$  and the atom, then perform a scattering of photon  $B$  against the atom, then to swap the atomic state back to photon  $A$ .

Although the construction of  $c\sigma_z$  through SWAP gates allows for direct interaction of  $|\psi_A\rangle$  with  $|\psi_B\rangle$ , it involves a total of  $3 + 1 + 3 = 7$  scattering interactions, which is significantly less compact than the three scatterings used in the construction from Ref. [3].

We can implement a more compact construction of  $c\sigma_z$  which also only requires three scatterings by using a measurement-based scheme shown in Figure S3. This second possible construction implements a  $c\sigma_z$  gate between photons  $A$  and  $B$  which is sandwiched between single-qubit gates. These extra gates can be implicitly removed by programming the single-qubit gate  $U_{\text{before}}$  which immediately precedes this operation to instead implement  $\left(Z_{\frac{\pi}{4}}B\right)^{-1} U_{\text{before}}$  and the gate  $U_{\text{after}}$  following  $c\sigma_z$  to implement  $U_{\text{after}} \left(BZ_{\frac{\pi}{4}}\right)^{-1}$ .

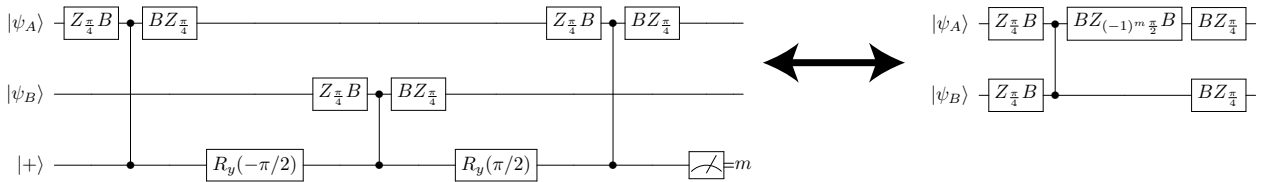


**Fig. S3.** Construction of a  $c\sigma_z$  gate with three scattering interactions using a measurement-based approach. After measurement, the left and right circuits are equivalent. The single-qubit gates on either side of  $c\sigma_z$  can be removed by absorbing them into the preceding/subsequent single-qubit gates as described above.

#### 5. CIRCUIT COMPILATION

An arbitrary  $n$ -qubit quantum operator  $U \in \text{U}(2^n)$ , can be compiled into a sequence of physical instructions on the proposed device using a three-step process shown in Figure 4 of the main text, and shown in greater detail in Figure S4

of this document. The first step is to decompose  $U$  into a sequence of single-qubit gates and  $c\sigma_z$  operations, a process described in our previous work [4]. The second step is to decompose each single-qubit gate via Euler angles as three  $R_y$  rotations which may be teleported onto the photonic qubits by a sequence of scatter-rotate-measure operations. The third step is to use a high-speed classical control system to modify the adaptive rotations which are applied to the atomic qubit based on the measurement outcomes during operation. Pauli errors which are accumulated during the course of the circuit operation can either be removed explicitly by scattering against  $|g_0\rangle$  or  $|g_1\rangle$ , as described at the end of Section 2, or can be removed implicitly (resulting in a more compact circuit) by programming the inverse of the error term into subsequent single-qubit operators. An example program for implementing a three-qubit quantum Fourier transform is shown in Program 1 at the end of this Supplementary Information document.

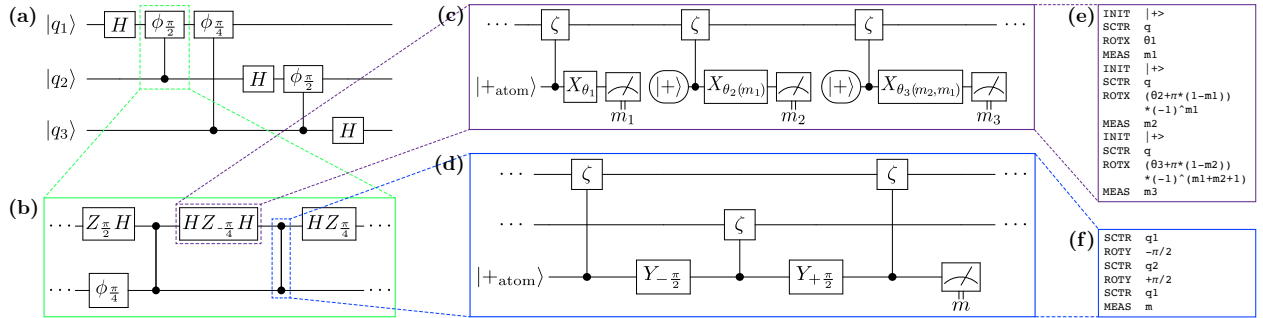


**Fig. S4.** Graphical depiction of the circuit compilation process. **(a)** The target quantum circuit we wish to implement in the device, in this case a three-qubit quantum Fourier transform. **(b)** The first step of the compilation process is to decompose complex circuit elements into single-qubit and  $c\sigma_z$  gates. The subcircuit depicted here implements the first controlled- $\phi_{\pi/2}$  gate between photonic qubits  $q_1$  and  $q_2$ . **(c, d)** The second step is to decompose each single-qubit gate (c) via Euler angles into a sequence of rotations which can be teleported from the atom to the photonic qubits, and to decompose each  $c\sigma_z$  gate (d) using the scattering sequence shown in Figure S3. **(e, f)** Programmatic representation of the instructions sent to the device to implement subroutines (c,d), respectively. The full code for implementing the target quantum circuit depicted in (a) is shown in Program 1.

## 6. IMPERFECTION ANALYSIS

Here we describe the details of the imperfection analysis that we used for estimating the achievable circuit depth, shown in Figure 4 of the main text. The main sources of error for our protocol are the same as for the Duan-Kimble protocol [3], but with the added loss from the switches and propagation loss through the storage ring. We group these errors into three main classes:

- **Pulse shape infidelity:** mismatch between the cavity output pulses for the atom being in the  $|g_0\rangle$  and  $|g_1\rangle$  states. This loss can be minimized by choosing the photon's temporal width ( $\tau$ ) to be much larger than the cavity photon lifetime  $1/\kappa$ :  $\kappa\tau \gg 1$ .
- **Spontaneous emission loss of the excited state of the atom,** where the atom in the  $|e\rangle$  state emits not into the desired cavity mode but into other modes or into free space. In our scheme, this causes photon leakage error when the atom is in the  $|g_1\rangle$  state, since the photon causes the  $|g_1\rangle$  state to temporarily transition to  $|e\rangle$ .
- **Photon loss due to optical elements.** This includes optical attenuation while propagating through the storage ring, insertion loss of the optical switches, and spurious loss from the cavity mirrors or the cavity medium.

We assume that the cavity mode at  $\omega_c$  is resonant with the atom  $|g_1\rangle \leftrightarrow |e\rangle$  transition frequency  $\Omega_1$ , since the detuning can be actively tuned to be zero, both in free-space by tuning the cavity length, as well as in solid-state nanophotonic systems through temperature or strain. We also assume that rotations of the atomic state by the cavity laser and measurement of the state via the quantum jump technique can be done with fidelity  $\mathcal{F} \approx 1$ , since both processes have been demonstrated experimentally with very high fidelities [5] greatly exceeding that of the effects listed above.

To quantify the effects of these sources of error, we assume the input waveguide contains a single photon Fock state of the form  $\int dt \phi_{\text{in}}(t) \hat{a}_{\text{in}}^\dagger(t) |\varnothing\rangle$ , where  $\phi_{\text{in}}(t)$  is the pulse shape,  $|\varnothing\rangle$  represents the vacuum state of the waveguide modes, and  $\hat{a}_{\text{in}}^\dagger(t)$  is a bosonic operator obeying the standard commutation relation  $[\hat{a}_{\text{in}}(t), \hat{a}_{\text{in}}^\dagger(t')] = \delta(t - t')$  which creates a photon propagating toward the cavity in the waveguide at time  $t$ . For the cavity output, we assume a similar form,  $\int dt \phi_{\text{out}}(t) \hat{a}_{\text{out}}^\dagger(t) |\varnothing\rangle$  [3, 6], where  $\hat{a}_{\text{out}}^\dagger(t)$  is similarly defined and creates a photon propagating away from the cavity at time  $t$ . For our analysis, we choose a Gaussian pulse envelope centered at  $t_0 = \Delta t/2$  for the input:  $\phi_{\text{in}}(t) \propto \exp[-(t - t_0)^2/\tau^2]$ , as studied in Ref. [3].

To solve for the output single-photon pulse, we use the analytical technique described by Shen and Fan [6, 7], which exactly solves the single-photon transport problem of a coupled atom-cavity-waveguide system, taking into account all relevant energy scales. The effective Hamiltonian of the overall system is given by [6]:

$$\begin{aligned} \mathcal{H}_{\text{eff}}/\hbar = & (\omega_c - i\kappa_i/2) \hat{a}^\dagger \hat{a} + (\Omega_e - i\gamma_s/2) |e\rangle\langle e| + \Omega_1 |g_1\rangle\langle g_1| + \Omega_0 |g_0\rangle\langle g_0| + (g \hat{a}^\dagger |g_1\rangle\langle e| + \text{H.c.}) \\ & + \int dx \delta(x) \left[ \sqrt{\kappa v_g/2} \hat{a}^\dagger \hat{a}_{\text{in}}(x) + \sqrt{\kappa v_g/2} \hat{a}^\dagger \hat{a}_{\text{out}}(x) + \text{H.c.} \right] \\ & + \int dx \hat{a}_{\text{in}}^\dagger(x) (\omega_c - i v_g \partial_x) \hat{a}_{\text{in}}(x) + \int dx \hat{a}_{\text{out}}^\dagger(x) (\omega_c + i v_g \partial_x) \hat{a}_{\text{out}}(x), \end{aligned} \quad (\text{S20})$$

where  $\hat{a}^\dagger$  is a bosonic operator that creates a photon in the cavity mode at  $\omega_c$  obeying  $[\hat{a}, \hat{a}^\dagger] = 1$ ,  $\kappa_i$  is the intrinsic dissipation rate of the cavity mode,  $\Omega_{0,1,e}$  are the energies of the respective atomic states,  $g$  is the single-photon atom-cavity coupling rate (equal to half the vacuum Rabi splitting),  $v_g$  is the group velocity of the waveguide in the vicinity of the cavity resonant frequency  $\omega_c$ , and  $\gamma_s$  is the spontaneous emission rate of the atomic  $|e\rangle$  state<sup>2</sup>. In the following analysis, we set  $\kappa_i = 0$ .

The spectrum of the output pulse,  $\tilde{\phi}_{\text{out}}(\omega) = \mathcal{F}\{\phi_{\text{out}}(t)\}$  is related to the input pulse spectrum  $\tilde{\phi}_{\text{in}}(\omega) = \mathcal{F}\{\phi_{\text{in}}(t)\}$  by the spectral response of the cavity-atom system  $R(\omega, g, \kappa, \gamma_s, |A\rangle)$ . Here,  $\mathcal{F}\{\cdot\}$  denotes the Fourier transform, and  $\omega$  denotes the input photon detuning from the cavity/atom resonance,  $\omega = \omega_{\text{in}} - (\Omega_e - \Omega_1) = \omega_{\text{in}} - \omega_c$ . The spectral response depends on the initial state of the atom  $|A\rangle \in \{|g_0\rangle, |g_1\rangle\}$ . This treatment captures the full quantum mechanical response of the system to a single-photon Fock state input for an arbitrary initialization of the atom, without making the semiclassical assumption of a weak coherent state for the input.

*Pulse shape infidelity and delay correction* — For an atom initialized as  $|A\rangle = |g_0\rangle$ , the response is identical to an empty cavity since the  $|g_0\rangle \leftrightarrow |e\rangle$  transition frequency is far-detuned from the cavity mode frequency  $\Omega_c$  [8]. In this case, the output pulse is slightly delayed from the input pulse by a time  $\delta t_0$ , as it couples into the empty cavity mode before coupling out, leading to a fidelity below unity, as shown in Figure 4 of the main text. For an initialization  $|A\rangle = |g_1\rangle$ , the photon is directly reflected from the front mirror of the cavity, since the dressed cavity modes are well-separated from the input photon frequency by the vacuum Rabi splitting for strong coupling  $g \gg \kappa, \gamma_s$ , and the delay  $\delta t_1 \approx 0$  is minimal. Here the pulse shape fidelity is defined as [8, 9]:

$$\mathcal{F}_{\text{shape}} \equiv \left| \int dt \tilde{\phi}_{\text{in}}^*(t) \tilde{\phi}_{\text{out}}(t) \right|, \quad (\text{S21})$$

where  $\tilde{\phi}_{\text{in}}$  and  $\tilde{\phi}_{\text{out}}$  are the renormalized input and output pulses. The pulse shape infidelity is defined as  $1 - \mathcal{F}_{\text{shape}}$ . Importantly, this quantity only describes the infidelity due to shape mismatch of the input and output pulses, not amplitude mismatch; the infidelity due to spontaneous emission loss is computed separately. The average infidelity for an initialization in the  $|+\rangle = (|g_0\rangle + |g_1\rangle)/\sqrt{2}$  state is calculated as the mean of the infidelities for the  $|g_0\rangle$  and  $|g_1\rangle$  states [3]. In our calculations, using a long pulse width  $\tau = 100/\kappa$  and total interaction timescale  $T = 500/\kappa$  and assuming no intrinsic losses in the cavity ( $\kappa_i = 0$ ) aside from spontaneous emission results in a low infidelity below  $10^{-3}$  per photon-cavity scattering event.

In Figure 4(b) of the main text, we plot the shape infidelity of various states as a function of the single-atom cavity cooperativity  $C \equiv 4g^2/\kappa\gamma_s$ , where  $\gamma_s$  measures the spontaneous emission rate and is fixed at  $\gamma_s = \kappa/5$ . The pulse shape infidelity of an interaction with the  $|g_1\rangle$  state decreases to negligible values as  $C$  increases, while the infidelity of  $|g_0\rangle$  reaches an asymptote at  $8 \times 10^{-4}$  due to the delay of the output pulse by a time  $\delta t_0$  which is independent of  $C$ ; the infidelity of the  $|+\rangle$  interaction asymptotes at  $4 \times 10^{-4}$ . Since the atom will usually be initialized to the  $|+\rangle$  state during operation of the device, it is useful to minimize the infidelity of interacting with this state. This can be done by delaying the reference pulse by a time difference  $t_{\text{delay}} = (\delta t_0 + \delta t_1)/2 \approx \delta t_0/2$  by adding an additional path length  $c t_{\text{delay}}/2$  to the top waveguide in Figure 1 of the main text. This distributes the infidelity due to the output pulse delay equally between the  $|g_0\rangle$  and  $|g_1\rangle$  states, such that the output pulse of a  $|g_1\rangle$  interaction is shifted forward by  $\delta t_0/2$  and the output of a  $|g_0\rangle$  interaction is delayed by  $\delta t_0/2$ . This results in an infidelity of approximately  $2 \times 10^{-4}$  which is independent of both cavity cooperativity (at  $C \gg 1$ ) and atomic state initialization.

*Spontaneous emission loss* — Atomic spontaneous emission noise from the excited  $|e\rangle$  state at a rate  $\gamma_s$  results in a partial loss of the photon, resulting in an output pulse with total photon number  $\int dt |\phi_{\text{out}}(t)|^2 < 1$ . We calculate the probability  $P_s$  of spontaneous emission loss as:

$$P_s = 1 - \frac{\int dt |\phi_{\text{out}}(t)|^2}{\int dt |\phi_{\text{in}}(t)|^2}. \quad (\text{S22})$$

<sup>2</sup>One should note that, while the use of the non-Hermitian  $-i\gamma_s/2|e\rangle\langle e|$  term is known to produce correct scattering matrices for single-photon interactions, the direct substitution of  $\Omega_e \rightarrow \Omega_e - i\gamma_s/2$  to describe spontaneous emission loss will yield incorrect results for temporally-overlapping multi-photon scattering interactions. [11] The more correct treatment here is to add additional couplings between the system Hamiltonian and a bath of modes describing the environment, but this is not necessary for our analysis, which is limited to single-photon interactions.

Spontaneous emission noise only applies to the  $|1\rangle \otimes |g_1\rangle$  component of the photon  $\otimes$  atom state. The atom will usually be initialized to the  $|+\rangle$  state, and averaging over possible input photon states, we obtain an average leakage probability of  $\bar{P}_s = P_s/4$ , as shown in Figure 4(b), which is well-approximated by  $\bar{P}_s = [4(1 + 2C)]^{-1}$ .

*Spurious photon loss and maximum circuit depth* — Finally, we account for loss due to propagation through the optical paths and switches as an average loss per cycle  $L$ . To estimate the maximum circuit depth  $D$  attainable with an overall fidelity  $\mathcal{F} > \mathcal{F}_{\text{target}}$ , we compute a “bulk fidelity” accounting for shape mismatch and loss due to average spontaneous emission and propagation through the storage ring. For simplicity, we assume the circuit operates on only a single photonic qubit and that the photon is scattered off the atom with every pass through the storage ring. The achievable circuit depth operating with success probability  $P_{\text{success}} = \mathcal{F}_{\text{target}}$  is thus the maximum  $D$  satisfying:

$$\left[ \mathcal{F}_{\text{shape}} \times (1 - \bar{P}_s) \times (1 - L) \right]^D \geq \mathcal{F}_{\text{target}}, \quad (\text{S23})$$

which is plotted as a function of cavity cooperativity and propagation loss in Figure 4(c) in the main text.

```

1 # Instruction set
2 # -----
3 # OPEN t ... open the switches at time t
4 # CLOS t ... close the switches at time t
5 # ROTX  $\theta$  ... laser pulse rotates atom state,  $R_x(\theta)$ 
6 # ROTY  $\theta$  ... laser pulse rotates atom state,  $R_y(\theta)$ 
7 # MEAS m ... measure atom state and store bit as m
8 # INIT  $\Psi$  ... initialize atom to  $|\Psi\rangle = |g0\rangle, |g1\rangle, |+\rangle$ 
9
10
11 # Scatter photon q and return it to ring
12 define SCTR q:
13     OPEN t_q- $\Delta t/2$       # t_q: time bin for |q>
14     CLOS t_q+ $\Delta t/2$     #  $\Delta t$ : temporal bin size
15     OPEN N* $\Delta t$ +t_q- $\Delta t/2$  # N: number of time bins
16     CLOS N* $\Delta t$ +t_q+ $\Delta t/2$  # N* $\Delta t$ : time around ring
17
18
19 # Explicitly correct Pauli errors after a gate
20 define CORR q m1 m2 m3:
21     if m3 == 0:
22         INIT |g1>
23         SCTR q
24         SCTR q
25         INIT |g0>
26         SCTR q
27     if m1 != m2:
28         INIT |g1>
29         SCTR q
30         SCTR q
31
32
33 # Single-qubit gate via Euler angles
34 define GATE q  $\theta_1$   $\theta_2$   $\theta_3$ :
35     INIT |+\rangle
36     SCTR q
37     ROTX  $\theta_1$ 
38     MEAS m1
39     INIT |+\rangle
40     SCTR q
41     ROTX  $(\theta_2 + \pi * (1 - m1)) * (-1)^{m1}$  # adaptive  $\theta_2$ 
42     MEAS m2
43     INIT |+\rangle
44     SCTR q
45     ROTX  $(\theta_3 + \pi * (1 - m2)) * (-1)^{(m1 + m2 + 1)}$ 
46     MEAS m3
47     CORR q m1 m2 m3 # remove Pauli  $\epsilon(m1, m2, m3)$ 
48
49
50 # Swap photon q with atom state
51 define LOAD q:
52     SCTR q
53
54     ROTX  $\pi$ 
55     ROTY  $\pi/2$ 
56     SCTR q
57     ROTX  $\pi$ 
58     ROTY  $\pi/2$ 
59     SCTR q
60     ROTX  $\pi/2$ 
61     ROTY  $\pi/4$ 
62
63 # Controlled- $\sigma_z$  between photons q1, q2
64 define CTRZ q1 q2:
65     GATE q1 0  $3\pi/4$   $-\pi/2$ 
66     GATE q2 0  $3\pi/4$   $-\pi/2$ 
67     SCTR q1
68     ROTY  $-\pi/2$ 
69     SCTR q2
70     ROTY  $+\pi/2$ 
71     SCTR q1
72     MEAS m
73     GATE q1 m* $\pi$   $\pi/2$   $(-1)^{m*3\pi/2}$ 
74     GATE q2  $\pi/2$   $3\pi/4$  0
75
76
77 # Run a 3-qubit QFT and measure the qubits
78 GATE q1 5.668 2.094 0.615 # H
79 GATE q1 3.757 2.094 5.668 #  $c\varphi(\pi/2)$ 
80 CTRZ q2 q1
81 GATE q1 2.101 1.718 4.182
82 CTRZ q2 q1
83 GATE q1 0.000 2.356 1.571
84 GATE q3 1.571 0.785 4.712 #  $c\varphi(\pi/4)$ 
85 GATE q1 4.712 2.356 0.000
86 CTRZ q3 q1
87 GATE q1 1.845 1.609 4.438
88 CTRZ q3 q1
89 GATE q1 5.918 2.283 1.041
90 GATE q2 5.668 2.094 0.615 # H
91 GATE q2 3.757 2.094 5.668 #  $c\varphi(\pi/2)$ 
92 CTRZ q3 q2
93 GATE q2 2.101 1.718 4.182
94 CTRZ q3 q2
95 GATE q2 0.000 2.356 1.571
96 GATE q2 5.668 2.094 0.615 # H
97
98 # State readout
99 LOAD q1
100 MEAS b1
101 LOAD q2
102 MEAS b2
103 LOAD q3
104 MEAS b3

```

**Program 1.** Assembly-like pseudocode for implementing the three-qubit quantum Fourier transform shown in Figure S4a. For simplicity and readability, this code explicitly corrects for Pauli errors using the CORR subroutine and removes extraneous  $BZ$  terms in the  $c\sigma_z$  gate construction using four additional GATE calls within CTRZ. The numerical values for the GATE angles in lines 78-96 were computed using a modified version of OneQubitEulerDecomposer in Qiskit [10].

## REFERENCES

1. Richard Jozsa, "An introduction to measurement based quantum computation," [arXiv:0508124](https://arxiv.org/abs/0508124) (2005).
2. C. Monroe, "Quantum information processing with atoms and cavities," *Nature* **416**, 238–246 (2002).
3. L. M. Duan and H. J. Kimble, "Scalable photonic quantum computation through cavity-assisted interactions," *Physical Review Letters* **92**, 127902 (2004).
4. Ben Bartlett and Shanhui Fan, "Universal programmable photonic architecture for quantum information processing," *Physical Review A* **101**, 042319 (2020).
5. Roger Gehr, Jürgen Volz, Guilhem Dubois, Tilo Steinmetz, Yves Colombe, Benjamin L. Lev, Romain Long, Jérôme Estève, and Jakob Reichel, "Cavity-Based Single Atom Preparation and High-Fidelity Hyperfine State Readout," *Physical Review Letters* **104**, 203602 (2010).
6. Jung Tsung Shen and Shanhui Fan, "Theory of single-photon transport in a single-mode waveguide. II. Coupling to a whispering-gallery resonator containing a two-level atom," *Physical Review A* **79**, 023838 (2009).
7. Jung Tsung Shen and Shanhui Fan, "Theory of single-photon transport in a single-mode waveguide. I. Coupling to a cavity containing a two-level atom," *Physical Review A* **79**, 059904 (2009).
8. L. M. Duan, A. Kuzmich, and H. J. Kimble, "Cavity QED and quantum-information processing with "hot" trapped atoms," *Physical Review A* **67**, 13 (2003).
9. L.-M. Duan, B. Wang, and H. J. Kimble, "Robust quantum gates on neutral atoms with cavity-assisted photon scattering," *Physical Review A* **72**, 032333 (2005).
10. Héctor Abraham *et al.*, "Qiskit: An open-source framework for quantum computing," (2019).
11. Eden Rephaeli and Shanhui Fan, "Dissipation in few-photon waveguide transport [Invited]," *Photonics Research* **1**, 110 (2013).